Cell Stem Cell
Resource

High-Throughput Screening Assay for the Identification of Compounds Regulating Self-Renewal and Differentiation in Human Embryonic Stem Cells

Sabrina C. Desbordes,[1,2,6,*] Dimitris G. Placantonakis,[2,5] Anthony Ciro,[3] Nicholas D. Socci,[4] Gabsang Lee,[1,2] Hakim Djaballah,[3] and Lorenz Studer[1,2,*]
[1]Developmental Biology Program
[2]Department of Neurosurgery
[3]High-Throughput Screening Core Facility
[4]Computational Biology Center
Memorial Sloan-Kettering Cancer Center, 1275 York Avenue, New York, NY 10021, USA
[5]Department of Neurological Surgery, Weill Cornell Medical College, 525 East 68th Street, New York, NY 10021, USA
[6]Present address: Differentiation and Cancer Program, Centre de Regulació Genòmica, C/Dr. Aiguader 88, 08003 Barcelona, Spain
*Correspondence: studerl@mskcc.org (L.S.), sabrina.desbordes@crg.es (S.C.D.)
DOI 10.1016/j.stem.2008.05.010

SUMMARY

High-throughput screening (HTS) of chemical libraries has become a critical tool in basic biology and drug discovery. However, its implementation and the adaptation of high-content assays to human embryonic stem cells (hESCs) have been hampered by multiple technical challenges. Here we present a strategy to adapt hESCs to HTS conditions, resulting in an assay suitable for the discovery of small molecules that drive hESC self-renewal or differentiation. Use of this new assay has led to the identification of several marketed drugs and natural compounds promoting short-term hESC maintenance and compounds directing early lineage choice during differentiation. Global gene expression analysis upon drug treatment defines known and novel pathways correlated to hESC self-renewal and differentiation. Our results demonstrate feasibility of hESC-based HTS and enhance the repertoire of chemical compounds for manipulating hESC fate. The availability of high-content assays should accelerate progress in basic and translational hESC biology.

INTRODUCTION

The availability of libraries of chemical compounds is a critical tool in drug discovery. High-throughput chemical screens have also become an important strategy to address questions in basic biology including stem cell research (Ding and Schultz, 2004). Recent studies have identified novel small molecules that mediate cell-fate acquisition and the differentiation behavior of a number of stem cell types. Examples include the following: self-renewal in mouse ES cells via dual inhibition of RasGAP and ERK1(Chen et al., 2006), neural (Ding et al., 2003) or cardiogenic (Wu et al., 2004a) specification of mouse ESCs, neurogenic response of neural stem/precursor cells by an orphan ligand, P-Ser (Saxe et al., 2007), or osteogenic differentiation in mesenchymal stem in response to purmorphamine (Wu et al., 2004b). Results from primary screens in mouse cells may often be applicable to similar cell populations of human origin. However, in the case of human ESCs (hESCs), this may not be the case given the distinct extrinsic signaling requirements to retain pluripotency in mouse (Ying et al., 2003) versus human (Vallier et al., 2005) ESCs.

hESCs self-renew extensively and give rise to various specialized cells relevant for modeling human development and for applications in regenerative medicine. While key transcription factors important for hESC renewal such as Oct4, Nanog, and Sox2 have been well characterized (Boyer et al., 2005; Ginis et al., 2004; Sato et al., 2003), extrinsic factors regulating hESC maintenance and early differentiation events are poorly understood (Hoffman and Carpenter, 2005). The development of high-content assays in hESCs has been challenging due to the difficulties in establishing suitable growth and plating conditions. Here we report the first HTS assay in hESCs and identify molecules that promote short-term self-renewal or drive early differentiation. Our data pave the way for the routine application of HTS assays in hESC biology and expand the repertoire of compounds available for manipulating hESC fate.

RESULTS

Adapting hESC Culture Conditions for HTS Platform

A critical step in the development of a robust hESC-based assay is the reproducible behavior of large-scale hESC cultures in a multiwell format. Prior to seeding in 384-well plates, hESCs were maintained under feeder-free conditions (Xu et al., 2001) and assessed for the expression of pluripotency markers (Figure 1A, see Figure S1 available online). To assure uniform cell distribution, we developed a single-cell dissociation protocol for hESCs by testing various enzymatic treatments and plating strategies (Figure S2). Accutase treatment resulted in fully dissociated cells suitable for plating on Matrigel-coated 384-well plates. Under these conditions, we observed a robust cell-density-dependent growth response as measured by Alamar blue at day 7 (Antczak et al., 2007; O'Brien et al., 2000) (Figure 1B). Plating of 6000 cells per well led to a density of hESCs suitable for automated microscopy and image analysis at 7 days after plating. At the time of

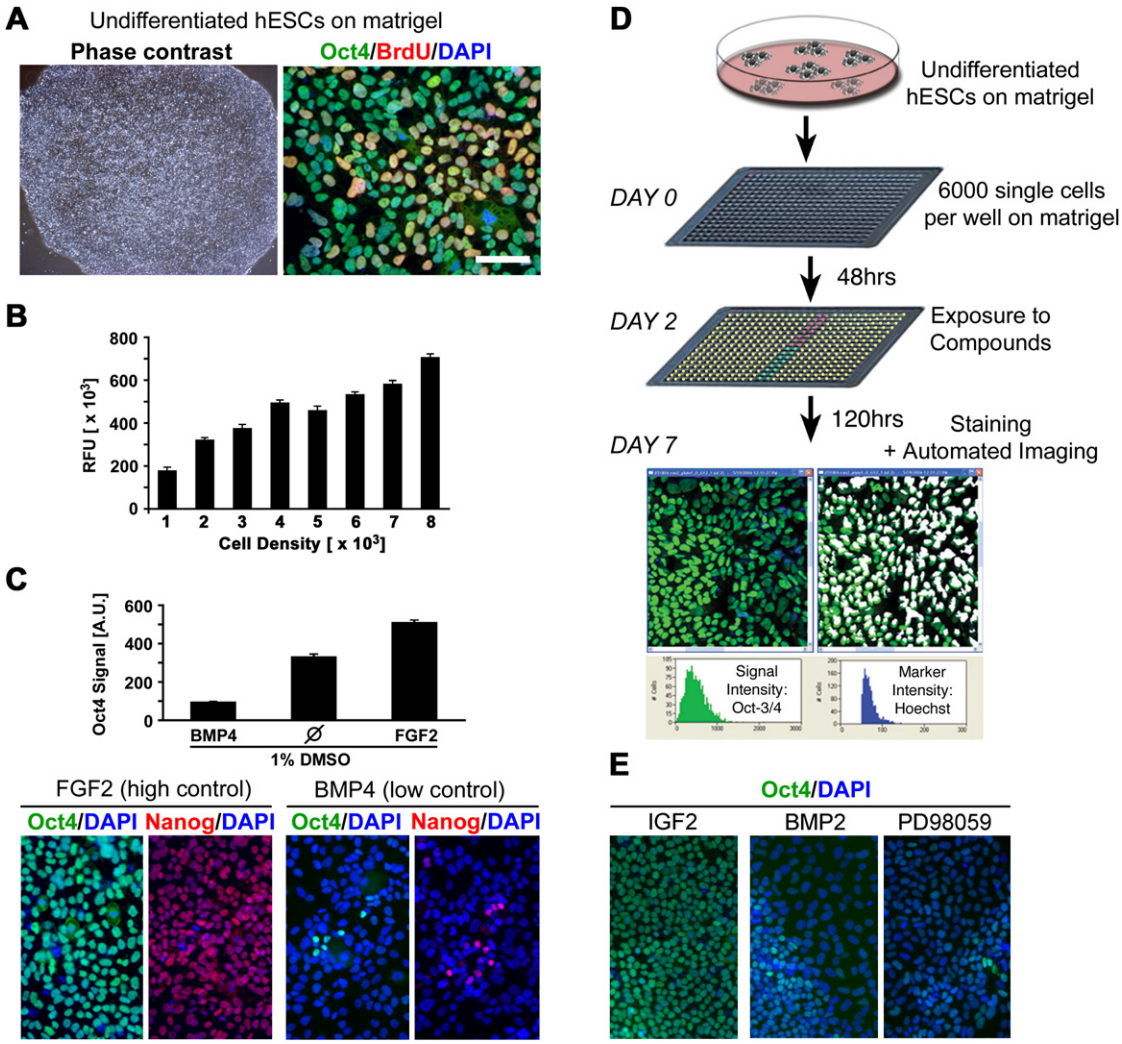

Figure 1. HTS Assay Development

(A) HESCs (H9 line) maintained on Matrigel prior to 384-well plating exhibit typical undifferentiated cell morphology (phase contrast), express Oct4, and incorporate the S phase marker BrdU.

(B) Cell titration on Matrigel-coated 384-well plates followed Alamar blue assay to determine the number of metabolically active cells (relative fluorescence units, RFU). Data are presented as mean ± SEM. Cell density refers to seeding density at the time of plating; Alamar blue is added at day 7, RFU is measured at day 8.

(C) (Upper panel) Quantification of Oct4 signal after treatment of hESCs in 384-well plates with BMP4 (low control) and FGF2 (high control). (Lower panel) Corresponding immunocytochemical analysis for Oct4 and Nanog in BMP4 and FGF2-treated cells. AU corresponds to arbitrary units. Data are presented as mean ± SEM.

(D) Schematic representation of HTS assay: undifferentiated hESCs were grown on Matrigel, dissociated into single cells using Accutase, and plated onto Matrigel-coated 384-well plates at a density of 6000 cells per well. After 48 hr, compounds (yellow) and high and low controls (red, FGF2; green, BMP4) were added for an additional 5 days. At day 7, automated immunocytochemistry for Oct4 was performed and signal intensity was quantified using automated laser-scanning confocal microscopy (GE InCell Analyzer 3000). The specific image shown corresponds to a culture well at day 7 after plating maintained in the presence of FGF2.

(E) Control experiments in HTS conditions were carried out using IGF2 for similar effect as FGF2 and BMP2 and PD98059 for loss of Oct4 expression. Scale bar in (A) corresponds to 500 μm in (A) (left panel), 50 μm in (A) (right panel), and 100 μm in (C) (lower panels) and in (E).

analysis, nuclei were separated from each other and cells were distributed evenly over the area of each well without forming multilayered structures (Figures 1C–1E). The density was also suitable to withstand repeated wash cycles required for our immunostaining protocol at the time of analysis.

Increase and decrease in the expression of the pluripotency factor Oct4 was used as primary readout. FGF2 supplementation was withdrawn from hESC cultures at day 2 after plating. Continued exposure to FGF2 until day 7 resulted in high Oct4 levels defined as high control (promoting self-renewal), while FGF2 withdrawal resulted in a sensitized state amenable to readout both self-renewal and differentiation compounds. Treatment with BMP4 induced a dramatic decrease in Oct4 expression, which was defined as low control (induction of differentiation) in our

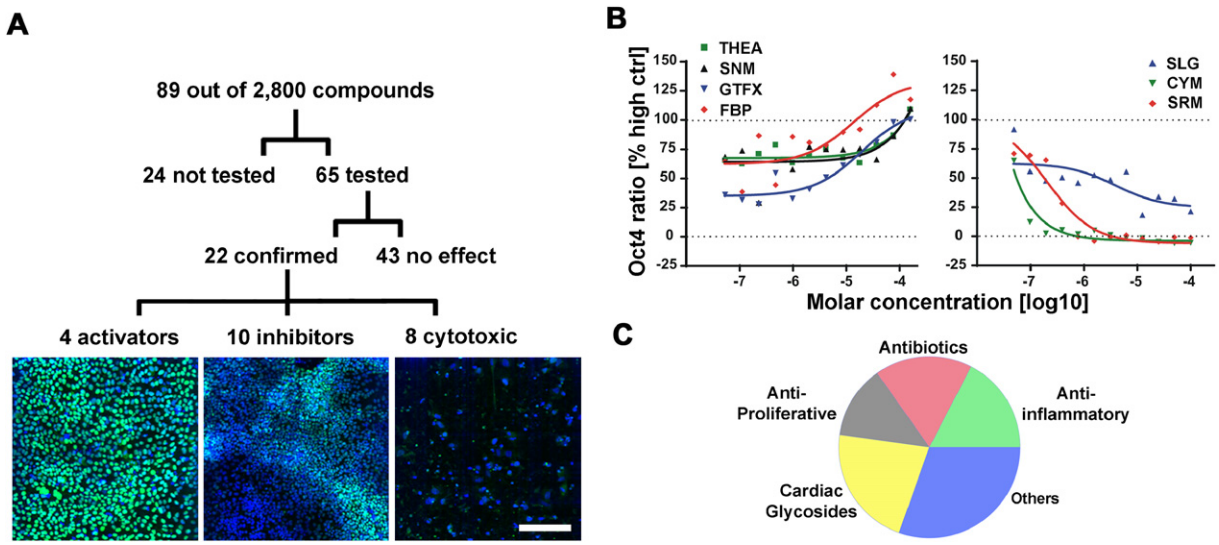

Figure 2. Results of 2880 Compound Library Screen

(A) (Upper panel) Out of 89 compounds identified in the primary screen, 65 compounds were subjected to further dose-response analysis resulting in 22 confirmed hits. (Lower panel) Representative images illustrating effects of activator, inhibitor, and cytotoxic compounds. Scale bar corresponds to 80 μm.

(B) Dose-response curves for a selected set of activators (left panel) and inhibitors (right panel). Data are expressed as Oct4 ratio of FGF2 versus BMP4-treated cells with FGF2 levels arbitrarily set at 100%. Levels of BMP4 and FGF2 treatment are marked in graph by dotted lines at 0% and 100%, respectively.

(C) The 22 chemicals with dose-dependent effects on hESC fate could be grouped into several categories based on current clinical drug indications of the compounds. Significant enrichment in hit list compared to library composition was observed for the categories cardiac glycosides ($p < 0.000001$) and antiinflammatory compounds ($p < 0.05$).

assay (Figure 1C). HESCs were exposed to the chemicals from days 2 to 7 (Figure 1D). Growth in conditioned medium (CM) for 48 hr prior to exposure to compounds provided sufficient time for dissociated hESCs to recover from the dissociation procedure and resume growth. The medium change at 48 hr after plating allowed removal of nonattached and dead cells. Compounds were diluted in KSR medium at a final concentration of 10 μM and added to the cells. Cells were assayed at day 7 (5 days/120 hr after exposure to the compounds) via high-throughput laser-scanning confocal microscopy (GE InCell Analyzer 3000) following automated immunocytochemistry. Oct4 levels were normalized to nuclear Hoechst 33342 staining in order to control for effects of the compounds on total cell number (Figure 1D), and z′ values were calculated to establish statistical robustness of the assay (Figure S3). To probe the validity of the 384-well assay, we tested a number of additional compounds with known activities in hESCs (Figure 1E) including IGF2 (Bendall et al., 2007), BMP2 (Pera et al., 2004), and PD98059 (Li et al., 2007). While our primary screen was carried out in H9 cells (WA-09), the conditions for single-cell dissociation, 384-well plating, and validations for high and low controls were fully reproduced in an independent hESC line (H1, WA-01; Figure S4).

Assay Validation and Primary Screen for Compounds Promoting hESC Self-Renewal and Differentiation

Using this assay, we screened a library of 2880 small molecules in multiple replicates. The library contained a broad set of biologically active and structurally diverse compounds including a set of 748 currently marketed drugs (for details, see the Experimental Procedures and Antczak et al. [2007]). Compounds were screened at a final concentration of 10 μM in a volume of 50 μl per well containing 1% DMSO (v/v). Normalized Oct4 values for each of the replicate 384-well plates were ranked and analyzed for repeated low or high hits. Out of the 89 hits (~3% of total molecules screened), 65 compounds were selected for subsequent dose-response assays based on their repeated high or low values in Oct4 expression intensity. A total of 22 compounds exhibited dose-dependent effects on normalized Oct4 values. Exposure to four of the compounds resulted in increased Oct4 intensity (activators), while ten compounds caused a decrease in Oct4 intensity (inhibitors) (Figure 2A). The remaining eight compounds showed dose-dependent toxicity in our assay without inducing differentiation (cytotoxic). A list of all 22 compounds is provided in Table S1. Representative images for each of the three responses (self-renewal, differentiation, cell death) are shown in Figure 2A, lower panel. Dose-response curves demonstrated that several activators induced Oct4 levels comparable to or higher than those achieved by FGF2 treatment. Similarly, several inhibitors led to a decrease in Oct4 levels comparable to BMP4 treatment (Figure 2B). Several classes of drugs were represented multiple times within the list of 22 confirmed hits, such as antiinflammatory drugs, antibiotics, and cardiac glycosides (Figure 2C). A significant overrepresentation of compounds in cardiac glycoside and antiinflammatory compound categories was observed compared with overall library composition: cardiac glycosides, 18% of confirmed hits, < 0.1% of library, $p < 0.000001$; antiinflammatory compounds, 14% of confirmed hits, ~4% of library, $p < 0.05$; antibiotics, 18% of confirmed hits, < 10% of library, p not significant. Chemical identity was confirmed by mass spectrometry (data not shown).

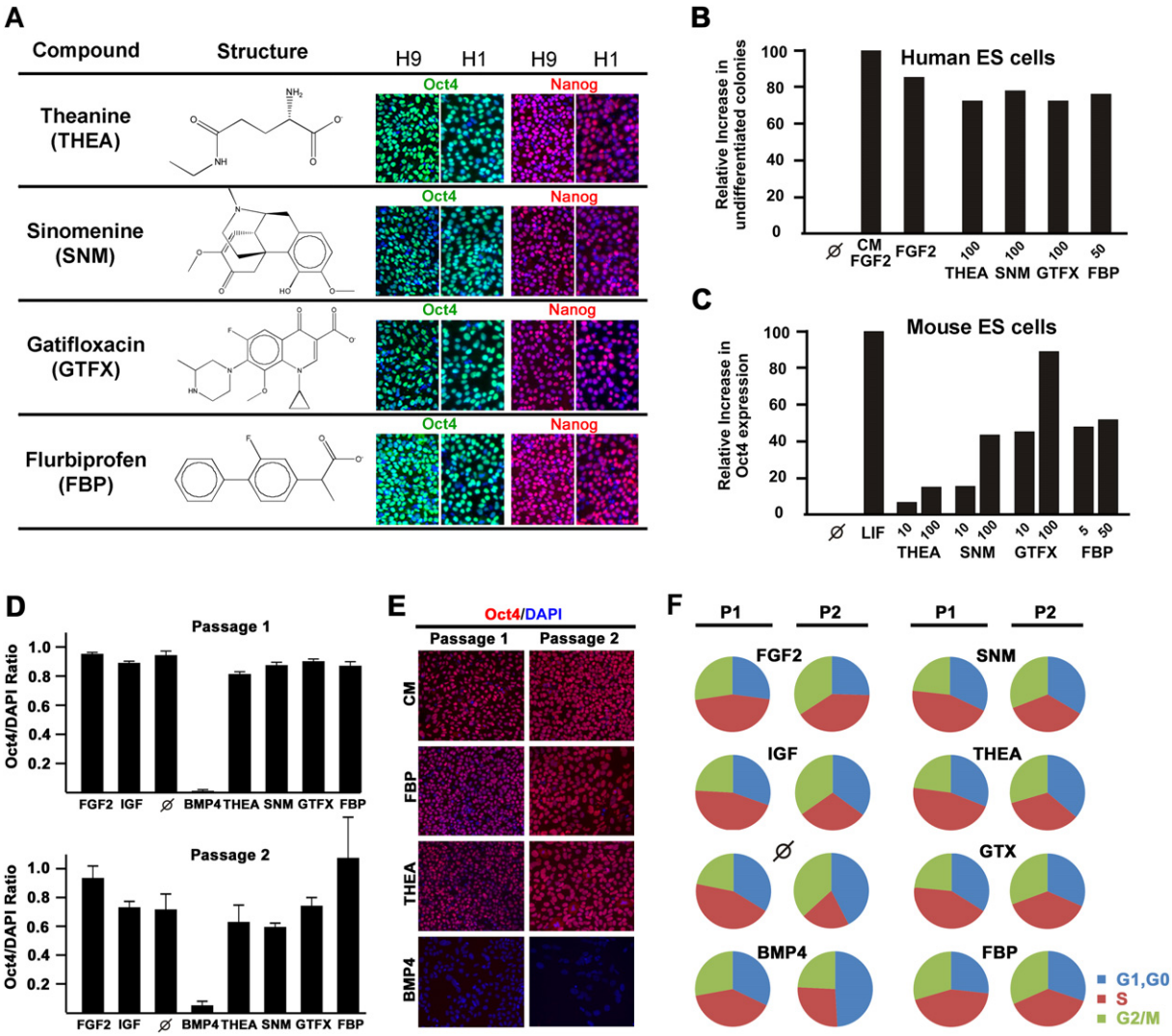

Figure 3. Small Molecules Promoting hESC Self-Renewal

(A) Expression of Oct4 and Nanog upon treatment with the four activator compounds was confirmed in H9 and in H1 hESCs.

(B) Repeated passaging of hESCs (H9) showed an increase in the percentage of undifferentiated colonies in presence of the self-renewal drugs, compared to HES medium alone (Ø). The graph represents the relative increase of undifferentiated colonies comparing HES medium alone (defined as 0%) versus MEF-CM supplemented with FGF2 (defined as 100%). Drug effects were tested at 50 and 100 μm as indicated.

(C) Mouse ESC self-renewal was tested after three passages using an *Oct4::eGFP* BAC transgenic mouse ESC line. The percentage of eGFP+ cells was quantified by flow cytometry, and the levels of Oct4 cells achieved in mouse ESC medium alone (defined as Ø = 0%) were compared to those treated with LIF (defined as 100%). Drug effects were tested at 10 and 100 μM as indicated.

(D) Quantification of the ratio of Oct4/DAPI staining under different culture conditions. Data are presented as mean ± SEM. Statistical analysis with ANOVA and post hoc Dunnett's test showed that the BMP4 group was significantly different from HES control ($p < 0.001$), while none of the other treatments were significantly different from control.

(E) Representative images of Oct4 immunoreactivity in hESCs maintained with CM, FBP, THEA, and BMP4 over two passages. Note that BMP4 causes a rapid downregulation of Oct4.

(F) Cell-cycle data for hESCs maintained with the self-renewal drugs or controls over two passages.

Secondary Assays Define Compounds with Effects on Oct4 Expression and Short-Term Self-Renewal in Human and Mouse ESCs

Activator compounds were subjected to a number of biological validations. Effects on Oct4 were confirmed using Nanog expression as an alternative pluripotency marker and using H1 as an additional hESC line. All four activator compounds, theanine (THEA), sinomenine (SNM), gatifloxacin (GTFX), and flurbiprofen (FBP) induced expression of Nanog at levels comparable to Oct4 in both H9 and H1 (Figure 3A). Maintenance of hESCs on Matrigel in the presence of these activators was tested in a basic hESC medium (Perrier et al., 2004) that lacked FGF2 supplementation and conditioning in mouse embryonic fibroblasts (MEFs). The number of undifferentiated colonies was quantified after multiple passages in vitro. We observed that each of the four activator compounds yielded a strong increase in the percentage of undifferentiated

colonies compared to cells maintained in hESC medium alone. The efficiency of these drugs in maintaining colonies undifferentiated was comparable to FGF2 exposure, though it did not reach the levels achieved by combined MEF conditioning and FGF2 supplementation of the medium (Figure 3B).

While key transcriptional regulators of pluripotency are shared between human and mouse ES cells, extrinsic conditions required to maintain an undifferentiated state are quite distinct. Here we tested whether the four activator compounds identified in our primary hESC based screen are capable of promoting self-renewal in mouse ES cells. To this end, an *Oct4::eGFP* line was generated by BAC transgenesis (Figure S5) following our previously published protocols (Tomishima et al., 2007). Using FACS analysis, we observed a dose-dependent effect of GTFX on Oct4 expression that was comparable to the effect of LIF treatment. Treatment with FBP or SNM resulted in a dose-dependent partial effect, while supplementation with THEA did not increase Oct4 expression in mouse ESCs (Figure 3C). We next assessed Oct4 expression in hESC cultures following initial exposure and subsequent passaging of cells under standard 6-well culture conditions. Oct4/DAPI ratio was determined following immunocytochemistry and quantitative imaging (ImageJ, for details see the Experimental Procedures). These data confirmed a near-complete loss of Oct4 in BMP4-treated cultures and maintenance of Oct4 expression in control, compound, and FGF2 treated cultures (Figures 3D and 3E). To further explore the impact of compound treatment on hESC growth, we performed cell-cycle analysis via flow cytometry using cells loading with propidium iodide-citrate solution (Figure 3F; for details, see the Experimental Procedures; Figure S6). The cell-cycle data showed that FGF2 treatment results in a high percentage of cells in S or G2/M phase, indicating a high degree of cell division at both passages (1 and 2). In contrast, exposure to BMP4 led to a marked increase in the proportion of cells in G1/G0 compatible with an increase in cell differentiation at passage 2. Drug-treated cells showed a high proportion of cells in S and G2/M phase, similar to IGF treatment. Cultures maintained under control conditions (Ø) yielded an increased proportion of cells at G1/G0 in passage 2.

A next set of studies addressed apoptotic cell death and maintenance of pluripotency in compound-treated hESC cultures. We observed low overall percentages of TUNEL+ cells at day 4 upon compound exposure without significant differences among the various treatment groups (Figure 4A). Directed differentiation assays toward neurectoderm (Perrier et al., 2004), endoderm (Watanabe et al., 2007), and mesoderm (Laflamme et al., 2007) fate showed that differentiation potential toward all three germ layers was retained (Figure 4B). However, long-term maintenance revealed that the drugs were not capable of reproducing the full effect of CM. Spontaneous differentiation under feeder-free conditions upon long-term passaging was eventually observed in all conditions, even when combining multiple compounds (data not shown).

Global mRNA expression analysis identified a total of >1000 transcripts (Table S2; Experimental Procedures) significantly regulated after drug treatment compared to basal hESC medium (without FGF2 or MEF conditioning). Gene expression analysis was performed immediately upon exposure to drugs (24 hr). At that stage of culture, we did not observe any signs of differentiation or cell heterogeneity. A heat map of the changes showed coregulation for many of the mRNAs induced by drug treatment with those induced by CM or CM supplemented with FGF2 (Figure 4C). Both SNM and GTFX showed highly significant overlaps in gene expression with CM treatment ($p < 10^{-9}$) and with combined CM + FGF2 treatment ($p < 10^{-16}$) (Figures 4D and 4E). Functional annotation of the most differentially regulated transcripts using DAVID, http://david.abcc.ncifcrf.gov (Dennis et al., 2003), confirmed strong regulation of TGF-β and Wnt signaling pathways in cultures treated with CM. However, despite significant overlap in overall analysis (Figures 4D and 4E), the top most differentially regulated categories in GTFX- or SNM-treated cultures were distinct (Figure 4F, Table S3). Regulation of heparin binding in GTFX-treated cultures could potentiate endogenous FGF signaling in hESC cultures. Fibronectin-1 that was significantly regulated in SNM-treated cultures has been a key component in a novel serum- and feeder-free culture system proposed for hESC maintenance (Amit and Itskovitz-Eldor, 2006). However, future studies will have to directly address the contribution of these individual candidate pathways in mediating the self-renewal-promoting response of each compound.

Interestingly, a chemical derivative of GTFX, orbifloxacin, had comparable effects on Oct4 maintenance, while another closely related compound, ciprofloxacin, lacked Oct4-inducing activities and caused differentiation toward mesendodermal fates (Figure S7). Similarly, we identified a derivative of FBP, felbinac, capable of promoting maintenance of Oct4 (Figure S7). The availability of related compounds with distinct action on hESC differentiation will provide an entry point toward structure-function studies and an understanding of mechanism of action. These data demonstrate that our HTS assay is suitable for the identification of compounds promoting hESC self-renewal and that several of these compounds fall into the category of currently marketed drugs (GTFX, SNM, and FBP) or natural compounds such as THEA found in black tea. The fact that none of the activators was sufficient to induce long-term self-renewal indicates the need for screening larger libraries and further modifications in screening design. One promising strategy may be the use of larger primary screens followed by stringent secondary assays measuring long-term hESC self-renewal more directly.

Induction of Distinct Lineage-Specific Markers in hESCs Exposed to Small Molecules Inhibiting Oct4 Expression

We next tested the function of a selected set of four out of ten inhibitor compounds including tretinoin (all-trans retinoic acid, RA), selegiline (SLG), cymarin (CYM), and sarmentogenin (SRM) that induced a dose-dependent reduction in Oct4 levels (Figure 5A). We first validated the effect of these drugs on loss of pluripotency using Nanog as an alternative marker in WA-09 and confirmed loss of both Oct4 and Nanog in H1 (Figure 5A). We hypothesized that loss of Oct4 expression in our high-content assay can be used as a surrogate marker for the identification of compounds that induce early differentiation events in hESCs. Key lineage choices accessible to undifferentiated hESCs include extraembryonic fates such as trophoblast (Xu et al., 2002) or primitive endoderm differentiation (Pera et al., 2004), mesendodermal (Barberi et al., 2007; D'Amour et al., 2005), and ectodermal fates (Zhang et al., 2001). A selected repertoire of these fate choices

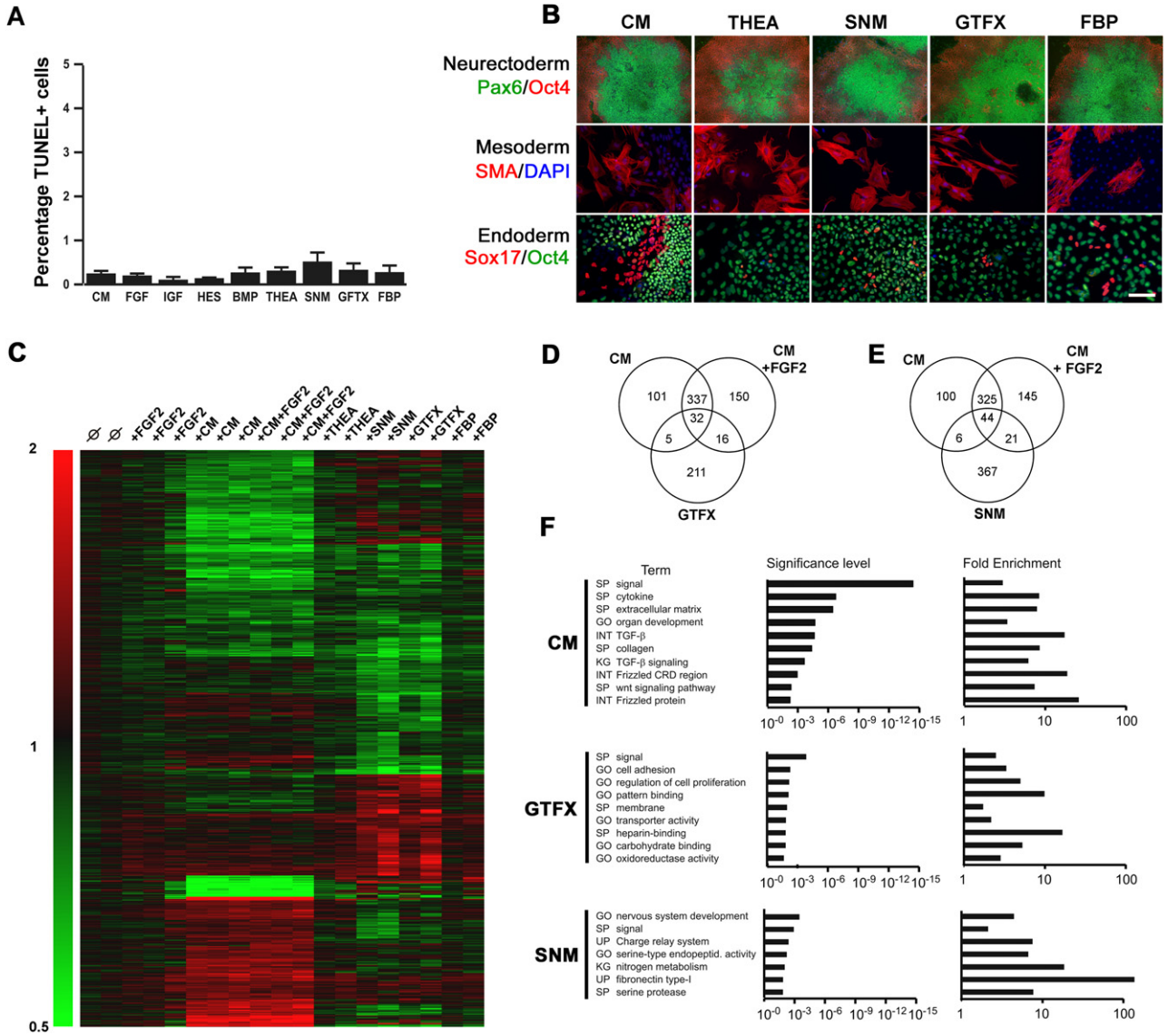

Figure 4. Functional Response and Potential Downstream Factors in hESCs Exposed to Candidate Self-Renewal Compounds

(A) TUNEL analysis of hESCs maintained in the presence of various compounds and under control conditions did not reveal significant differences among groups. Data are presented as mean ± SEM.

(B) Pluripotency was assessed using directed differentiation protocols in hESCs maintained for three passages in the presence of compounds or control conditions.

(C) Total of 1,145 transcripts out of 22,177 transcripts were differentially expressed during treatments of hESCs with CM, CM + bFGF, or self-renewal drugs compared to basal hESC medium alone. These genes were clustered, and a heat map for all conditions in duplicate or triplicates was established.

(D) Venn diagram showing the number of transcripts differentially expressed in GTFX-treated cells or cells maintained in MEF-CM or in MEF-CM supplemented with FGF2 (CM + FGF2) versus cells maintained in basic hESC medium. Significance of overlap in GTFX versus CM was $p < 10^{-10}$; GTXF versus CM + FGF2 was $p < 10^{-16}$.

(E) Venn diagram showing the number of transcripts differentially expressed in SNM-treated cells using the same parameters as in (D). Significance of overlap in SNM versus CM was $p < 10^{-10}$ and $p < 10^{-16}$ versus CM + FGF2.

(F) Functional annotation analysis using DAVID platform (http://david.abcc.ncifcrf.gov; Dennis et al., 2003) illustrates overrepresentation of transcript categories within a given treatment group compared to control cultures. Significance and relative fold levels of enrichment are presented. Full description of the algorithms used, the definition of the categories, and list of all transcript members included per category are provided in Table S3 and in the Experimental Procedures.

was assessed at the time of Oct4 analysis by automated immunocytochemistry for cytokeratin 18 (CK18, trophoblast marker), Sox17 (mesendoderm/endoderm), and Pax6 (neuroectoderm). We observed that exposure to tretinoin induced CK18 at levels comparable to BMP4 treatment. Exposure to the cardiac glycosides (CYM or SARM) caused an increase in Sox17 expression (Figure 5B). Quantification of the percentage of Sox17+ cells (Figures 5C and 5D) was compatible with the Sox17 signal intensity data in Figure 5B. Both CYM and SARM yielded an increase in the percentage of Sox17+ cells comparable to the effect

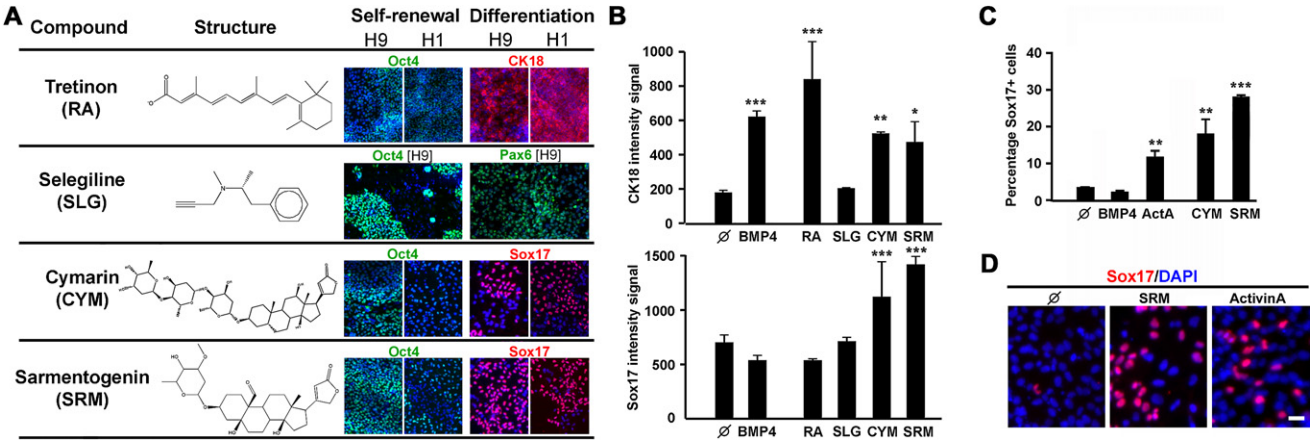

Figure 5. Small Molecules Driving hESC Differentiation

(A) Expression of Oct4 was downregulated upon treatment with inhibitor compounds (left panels). Markers of differentiation were used to characterize lineage choice promoted by a given compound. Tretinoin (RA) showed strong induction of cytokeratin 18 (CK18), selegiline increased expression of Pax6 over time, and cymarin and sarmentogenin showed induction of Sox17 (right panels). These effects were established in the hESC line H9 and confirmed in H1.

(B) (Upper panel) CK18 intensity signal was quantified using the confocal InCell Analyzer 3000 at day 7 of assay. (Lower panel) Under the same conditions, expression of Sox17 was quantified. Data are presented as mean ± SEM. Statistical significance was defined as: *$p < 0.05$, **$p < 0.01$, ***$p < 0.001$, ANOVA followed by Dunnett's test.

(C) Percentage of Sox17+ cells under control conditions or in the presence of CYM, SRM, or ActivinA (positive control).

(D) Representative images of Sox17 immunocytochemistry at the time of analysis used for quantification in (C). Scale bar in (D) corresponds to 10 μm.

observed upon ActivinA exposure. While SLG did not show any significant increase in the percentage of cells expressing differentiation markers at day 7 of differentiation, an increased number of Pax6+ clusters in longer term cultures is compatible with recent observations in mouse ES cells (Esmaeili et al., 2006).

Global gene expression analysis 24 hr after drug exposure (Figure 6A) confirmed a large number of differentially expressed transcripts (Table S4) that are significantly coregulated in CYM- and SRM-treated cultures (Figure 6B; $p < 10^{-241}$). A large number of these transcripts were compatible with early differentiation events toward mesendodermal lineage choice. In contrast, exposure to tretinoin (RA) treatment led to an upregulation of genes compatible with extraembryonic and neuroectodermal differentiation (Figure 6C, Table S4), while transcripts induced by SLG treatment were most compatible with neurectodermal and neural crest differentiation (Figure S8). Functional annotation analysis (DAVID, http://david.abcc.ncifcrf.gov/; Dennis et al., 2003) in RA-treated cultures demonstrated enrichment in categories known to be associated with retinoid signaling including regulation of Hox genes, modulation of Id2 repressor, and other bHLH-related factors (Figure 6D). SLG exposure showed significant enrichment in transcripts associated with signaling and cell differentiation. SRM and CYM exposure showed enrichment in the regulation of highly overlapping sets of functional category terms including lipoprotein, basic leucin zipper, and various categories associated with development and differentiation (Figure 6D, Table S5).

DISCUSSION

Our data demonstrate the feasibility of performing a primary HTS assay in hESCs and pave the way for establishing high-content screening platforms ranging from assays that address questions in basic hESC biology to translational applications and drug discovery. The design of our primary HTS assay is suited for the screening of large compound libraries. The significant costs of such an effort may be offset by the identification of compounds promoting self-renewal as well as compounds driving differentiation. Putative differentiation compounds identified in the primary screen can be subsequently classified into compound classes promoting various lineage-specific cell fates using secondary screens. However, it will be critical in the future to fully validate all secondary screens using z′ analysis up to the standards of a primary screen. Our current assay requires high initial plating densities to compensate for cell loss at the time of plating and to assure even cell distribution throughout the surface area of each well. At this cell density, we did not observe stacking of multiple nuclei that would prevent reliable image analysis. One disadvantage of using such high cell densities is the relatively large number of total cells needed for a full-scale HTS screen. For example, screening a library of 1 million compounds without replicates but including internal high and low controls will require $\sim 6 \times 10^9$ cells. Future studies should allow primary HTS assays in hESCs at lower cell densities by reducing initial cell death at plating. One interesting compound to be tested is the ROCK inhibitor Y-27632, shown to increase efficiency of plating dissociated hESCs at low cell densities (Watanabe et al., 2007).

There is currently a very limited set of chemical compounds available that affect hESC behavior (Chen et al., 2006; Ding et al., 2003; Sato et al., 2004), and none of these compounds have been identified through primary HTS assays in hESCs. The newly discovered compounds enhance our repertoire of chemical modulators suitable for directing growth and differentiation of hESCs. Future studies will have to explore the mechanistic action of these compounds on the self-renewal and differentiation machinery of hESCs. Our gene expression data, functional annotation analysis, and data from the literature on drug action of several of these compounds will provide

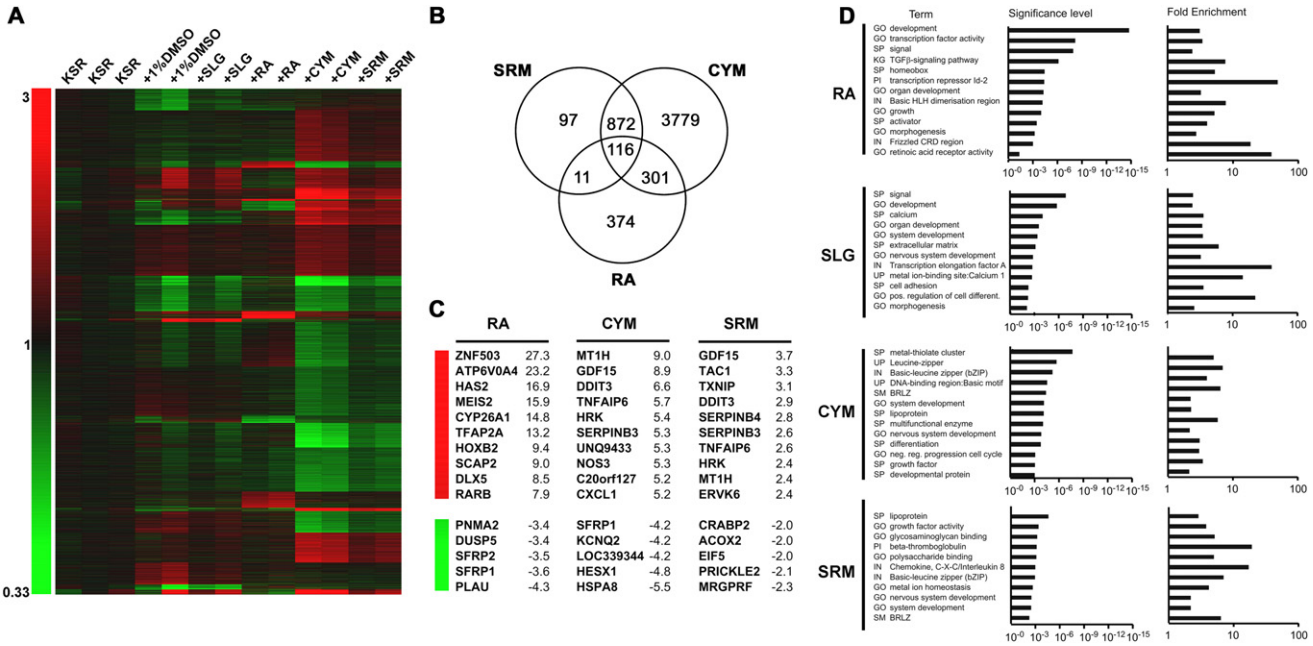

Figure 6. Potential Downstream Mediators in the Response of hESCs to Differentiation Compounds

(A) A total of 6163 transcripts were differentially expressed during treatments of hESCs with KSR+DMSO or treatment with any of the inhibitor compounds compared with cells maintained in KSR medium alone. These genes were clustered, and a heat map for all conditions in duplicate or triplicates was established.

(B) Venn diagram showing the number of transcripts differentially expressed in sarmentogenin (SRM), cymarin (CYM), or tretinoin (RA) versus cells maintained in KSR only.

(C) The top ten upregulated and top five downregulated genes out of the total set of 22,177 transcripts are listed for the three drugs. Six out of the ten most regulated transcripts in CYM and SRM are identical.

(D) Functional annotation analysis using DAVID platform (http://david.abcc.ncifcrf.gov/; Dennis et al., 2003) illustrates overrepresentation of transcript categories within a given treatment group compared to control cultures. Significance and relative fold levels of enrichment are presented. Full description of the algorithms used, the definition of the categories, and a list of all transcript members included per category are provided in Table S5 and in the Experimental Procedures.

valuable entry points to this end. One issue to be addressed is whether any given compound works directly on undifferentiated hESCs or whether such an effect could be due to a bystander effect mediated by hESC-derived differentiated progeny. Such a bystander effect could feed back on undifferentiated hESCs as proposed in the case of spontaneously emerging hESC-derived fibroblast (Bendall et al., 2007). The lack of true long-term self-renewal factors among the activator compounds identified in the current study suggests that such molecules may be rare and require the screening of much larger libraries. Another critical question is whether the induction of Sox17 observed upon exposure to CYM and SRM can be translated into a protocol for generating endodermal derivatives from hESCs. While the percentage of Sox17+ cells was increased at levels comparable or higher than those achieved by ActivinA, CYM and SRM had a negative effect on overall cell growth. Future studies will have to address this issue in more detail by systematically mapping the expression of endodermal genes and cell fates in the presence of these compounds.

Several of the cytotoxic factors identified here (Figure 2A, Table S1) could be further explored for the selective elimination of undifferentiated hESCs intermixed in hESC progeny prior to transplantation and as a paradigm for cell-toxicity studies. In addition, one direct application for such assays could be the identification of compounds with teratogenic potential. Differentiation of self-renewal promoting effects at the hESC stage may reflect the potential for similar effects during early human embryonic development in vivo. The identification of retinoic acid, a well-known teratogenic compound in our study, supports this hypothesis. The emergence of national HTS centers such as the ten centers established through the National Institutes of Health (NIH) Roadmap Initiative http://mli.nih.gov/mli/mlscn/screening-centers/ and additional centers sponsored by state initiatives in the U.S. and multinational initiatives in Europe and Asia should provide access to HTS technology more readily. This will be particularly important for users in the stem cell field that do not have access to individual screening centers at their own institutions. Once an HTS assay has been optimized for use, which represents the longest step, the actual screening process is quite rapid. The cell numbers required for our assay (50–100 × 10^6 cells) can be generated starting from a single 6 cm plate of hESCs in approximately 4 weeks. From the time of plating to full data analysis of a 2880 compound library, the screen can be completed in less than 2 weeks. There was an overall failure rate of about one in three assays defined as not reaching acceptable standards in positive and negative controls that are included on every plate (value not comparable to original z′). This relatively large failure rate was caused mainly by the variability in the quality of undifferentiated hESCs maintained in bulk cultures. Future improvements in large-scale hESC culturing should help reduce failure rates.

In conclusion, our data demonstrate the feasibility of performing primary HTS assays in hESCs. Our screen resulted in the

identification of novel compounds for manipulating hESC fate. The use of HTS assays should dramatically enhance our understanding of hESC biology and facilitate the application of hESCs in drug development and cell therapy.

EXPERIMENTAL PROCEDURES

Human ES Cell Culture and 384-Well Plating

The hESC lines H9 (WA-09, passages 35–45) and H1 (WA-01, passages 30–45) were used for this study. HESCs were cultured on mitotically inactivated MEFs as described previously (Perrier et al., 2004) followed by feeder-free growth on Matrigel in MEF-CM (Xu et al., 2001) prior to 384-well plating. For 384-well plating, cells were harvested following Accutase dissociation for 20 min at 37°C. At that stage, single-cell suspensions could be obtained without further mechanical dissociation, and dissociated cells displayed high levels of viability (>95% based on trypan exclusion). hESCs were plated at 6000 cells per well from a stirred single-cell suspension (typically 50–100 × 10^6 cells per experiment) in MEF-conditioned hESC medium using a Multidrop Dispenser (Thermo). Quality control (QC) steps were added with each set of experiments using Alamar blue assay. For the assay, the dye resazurin was added to living hESCs at 5 μM according to the specification of the manufacturer, and fluorescence was measured 24 hr later, providing a quantitative estimate of the number of metabolically active cells. At the time of the assay (day 2 of assay), KSR medium (Perrier et al., 2004) was added to the plates of compounds diluted in 100% DMSO, and the KSR-diluted compounds were transferred to the hESC plates at 10 μM final concentration in 1% DMSO (v/v). The cells were maintained in compounds until day 7. DMSO is the preferred solvent for chemical libraries because of its stability and low-temperature flash point, making it amenable for use with robotic liquid handling systems. To address potential interference of DMSO with hESC self-renewal, we demonstrated robust long-term maintenance of undifferentiated hESCs in the presence of 1% DMSO when using CM + FGF2 (10 ng/ml). These studies were based on measuring expression of pluripotency markers (Oct4, SSEA3), cell-cycle analysis, and percentage of undifferentiated colonies over a period of 5–10 passages (data not shown).

Every 384-well plate in the screen included 16 wells each for high and for low internal controls. FGF2 (R&D Systems) was supplemented at 200 ng/ml (Levenstein et al., 2006) in high control wells (promoting self-renewal). BMP4 (R&D Systems) was added at 200 ng/ml in low control wells (induction of differentiation). These concentrations were selected based on dose titration assays for high and low Oct4 signal under HTS conditions, taking into account stability and degradation pattern of the factors (data not shown). Additional control treatments were used to demonstrate the robustness of the assay: IGF (30 ng/ml, R&D Systems), BMP2 (100 ng/ml, R&D Systems), and PD98059 (50 μM, Tocris Bioscience).

Immunohistochemistry, Automation, and Image Analysis

Fixation in 4% paraformaldehyde/0.15% picric acid was followed by standard fluorescent immunocytochemical techniques using the following primary antibodies: monoclonal, BrdU (Sigma) and Oct4 (Santa-Cruz); and polyclonal, Nanog (R&D Systems), Sox17 (R&D Systems), CK18 (Santa-Cruz), and Pax6 (Covance). All stainings were adapted for 384-well plates for automation. Liquid-handling systems were used to aspirate and dispense liquid from and in 384-well plates. Aspirations were performed using a Multidrop 384 (Thermo, Electron Corporation, Waltham, MA). Dispensions of fluids were performed using either the Multidrop 384, for rinsing steps, or a Flexdrop IV (PerkinElmer, Waltham, MA) for Matrigel (BD Biosciences, San Jose, CA), cell plating, and antibody staining. Compounds were transferred on cells using a TPS-384 total pipetting platform (Apricot). Confocal image acquisition was carried out with an InCell Analyzer 3000 (GE Healthcare). An average of four images per well were collected, two images at 488 nm and two images for Hoechst 33342, using a 10× objective. Data analysis was performed using the InCell Investigator software. Images were first processed by a flat-field correction. The object intensity analysis module from the InCell Investigator software (GE Healthcare, USA) was used to measure the signal intensity of objects in the defined measurement region. The algorithm first identified the nucleus in the marker channel and then quantified the signal region within the area of the nucleus. Average signal intensity was calculated by measuring total intensity divided by the number of objects (i.e., cells) and expressed as arbitrary units (AU). Screening data files obtained from the Amersham InCell Investigator software postprocessing were loaded into the HTS Core Screening Data Management System (Antczak et al., 2007). Hits were defined as the repeated top ranked compounds per plate that also exhibited at least a >30% increase (inducing compounds) or >30% decrease (inhibitory compounds) in normalized Oct4 values in ≥2 independent runs in duplicates. Data for some compounds data were confirmed in up to six independent runs.

Validation Studies

Self-Renewal Compounds

The effect was tested over multiple passages on undifferentiated H9 hESCs passaged using a standard dispase (Worthington Biochemical Corp., Lakewood, NJ) protocol (Perrier et al., 2004) under feeder-free conditions on Matrigel in the presence of MEF-CM and FGF2 (10 ng/ml). Two days after plating, CM was replaced with HES medium containing THEA (50 μM), SNM (50 μM), FBP (25 μM), or GTFX (50 μM). Control conditions were matched with regard to DMSO concentration. At each passage, cells were dissociated with Accutase and subjected to cycle analysis by FACS after propidium iodide-citrate solution treatment (50 μg/ml propidium iodide, 0.1% sodium citrate dihydrate, 200 μg/ml RNaseA, and 0.1% Triton X-100). In brief, 2 × 10^5-dissociated hESCs were washed once with PBS, incubated with propidium iodide-citrate solution for 10 min in the dark, and analyzed. FACS analysis was performed on a FACSCalibur system (BD Biosciences). For Oct4/DAPI ratio quantification, cells were subjected to Oct4 immunocytochemistry, and four 0.15 mm^2 microscopic fields were imaged and analyzed using ImageJ software (NIH, Bethesda, MD). In brief, Oct4 and DAPI channels were subjected to thresholding independently, the stain surface area was measured, and finally the ratio of the surface areas was calculated. Apoptotic cell death was quantified after plating of H9 hESCs on Matrigel in CM + FGF2 (10 ng/ml) for 2 days followed by 4 days of drug treatment and subjection to fixation and TUNEL assay (Roche Diagnostics Corporation, Indianapolis, IN). The percentage of TUNEL+ cells was quantified in uniform randomly selected fields of 0.15 mm^2 (n = 5 per group) together with DAPI for ratio measurement. Pluripotency was assessed by directed differentiation of H9 maintained over three passages in the presence of self-renewal compounds. For endoderm induction, hESCs were treated with ActivinA (100 ng/ml) for 6 days in DMEM/F12 medium containing 1% FBS (Invitrogen, Carlsbad, CA) as previously described (Watanabe et al., 2007). For mesoderm induction, cells were cultured in RPMI medium supplemented with B27 (Invitrogen) as previously reported (Laflamme et al., 2007). In brief, ActivinA (100 ng/ml; R&D Systems) was added for 1 day, followed by BMP4 (10 ng/ml) for an additional next 4 days. After withdrawal of BMP4, cells were maintained in RPMI-B27 medium for 12 days before staining. Neuroectoderm induction was achieved using a coculture system (Perrier et al., 2004) in which hESCs are plated on stromal cells (MS5) in the presence of Noggin (250 ng/ml) added starting at day 3 of differentiation. Immunofluorescence analysis was performed at day 12 of differentiation. The following antibodies were used: Sox17 for endoderm induction, smooth muscle actin (SMA, Sigma) for mesodermal differentiation, and Pax6 (Covance) for neuroectoderm induction.

Differentiation Compounds

hESCs were plated in 384-well plates following the described HTS protocol. Each condition (untreated medium Ø, BMP4, RA, SLG, CYM, SRM, or ActivinA) had six replicates for each staining (CK18 or Sox17). Four images per well were captured by InCell 3000 scanner and quantified for intensity signal measurements. Percentages of Sox17+ cells were quantified by computer-assisted analysis using ImageJ with automated thresholding as described above. All data were normalized to Hoechst (intensity signal) or DAPI (percentage of Sox17+ cells).

Chemical Libraries

The library used for the current study combines chemicals obtained commercially from Prestwick and MicroSource. The MicroSource library (http://www.msdiscovery.com/) contains 2000 biologically active and structurally diverse compounds from known drugs, experimental bioactives, and pure natural products. The library includes a collection of 720 natural products and their derivatives, a range of simple and complex oxygen-containing heterocycles,

alkaloids, sesquiterpenes, diterpenes, pentacyclic triterpenes, sterols, and many other diverse representatives. The Prestwick Chemical Library (http://www.prestwickchemical.fr/) is a collection of 880 high-purity chemical compounds selected for structural diversity and representing drug classes with a broad spectrum of therapeutic uses. More than 85% of its compounds are marketed drugs.

Statistical Analysis of HTS Assay and Dose-Response Study

To assess the performance of the assay, the z′ factor value was determined. This factor represents a dimensionless parameter, which value can range between <0 and 1. It is defined as $1 - z' = (3\sigma c^+ + 3\sigma c^-)/|\mu c^+ - \mu c^-|$, where σc^+, σc^-, μc^+, and μc^- are the standard deviations (σ) and averages (μ) of the high (c^+) and low (c^-) controls (Zhang et al., 1999). To obtain this value, three 384 plates of high control (1% DMSO + FGF2) and low controls (1% DMSO + BMP4) were analyzed (Figure S3). For dose-response analysis, each 384-well plate of exposed to hits from the primary screen contained replicate wells for high and low controls. Each concentration was applied in duplicates over a range of 12 different doubling dilutions between 0 and 100 μM.

Microarray Analysis

RNA was isolated (QIAGEN), labeled, and prepared for Illumina bead arrays following the instructions of the manufacturer (SKI Genomics Core Facility). All data were analyzed using the Bioconductor packages (http://www.bioconductor.com/) for the R statistical system. The arrays were quantitated using the Illumina BeadStudio program, and raw data (normalized and non-background subtracted signal levels) were exported. Normalization was carried out using the quantile method for the AFFT Bioconductor package. Probes that had detection p values >0.01 in 75% or more samples were removed as noise. Expression signal levels were then log 2 transformed. To determine genes that are differentially expressed between the various sample types, the LIMMA package was used. This performs a variant of linear models (t test or ANOVA) in which the variance is corrected to deal with small sample numbers. To account for the multitesting issue, the false discovery rate (FDR) method was used with cutoffs of 0.20 for the HES samples comparison (self-renewal factors) and 0.05 for the KSR sample comparison (differentiation factors). To determine the significance of overlaps between different gene sets, the standard Fisher's test (hypergeometric distribution) was performed.

Functional annotation analysis was performed using the DAVID platform (DAVID, http://david.abcc.ncifcrf.gov/ [Dennis et al., 2003]). A list of differentially regulated transcripts for a given compound was established at the FDR levels described above. For analysis, we selected only transcripts with a fold change of $\geq$2 compared with control. For those compounds with less than 200 differential transcripts at a fold change level of 2, the analysis was extended to those with a fold change of $\geq$1.5. Final selection of categories for presentation eliminated duplicate categories that contained identical gene lists. Furthermore, all included terms exhibited significant p values for enrichment and generally contained greater than two members per category.

ACCESSION NUMBERS

All raw data are available online under Gene Omnibus (GEO) accession number GSE11302.

SUPPLEMENTAL DATA

Supplemental Data include eight figures and can be found with this article online at http://www.cellstemcell.com/cgi/content/full/2/6/602/DC1/.

ACKNOWLEDGMENTS

We thank the members of the Memorial Sloan-Kettering Cancer Center High-Throughput Screening (MSKCC HTS) Core Facility for their help during the course of this study, especially C. Radu, D. Shum, and G.E. Sanchez. We also thank V. Tabar, Y. Elkabetz, M. Tomishima, F. Lafaille, and H. López-Schier for critical comments on the manuscript and S. Gong and N. Heintz for providing the *Oct4::eGFP* BAC. Supported by National Institute of Neurological Disorders and Stroke (NINDS) grant (R21NS44231), The Starr Foundation, Mr. W.H. Goodwin and Mrs. A. Goodwin and the Commonwealth Foundation for Cancer Research, The William Randolph Hearst Foundation, and The Experimental Therapeutics Center of MSKCC.

Received: September 12, 2007
Revised: April 1, 2008
Accepted: May 13, 2008
Published: June 4, 2008

REFERENCES

Amit, M., and Itskovitz-Eldor, J. (2006). Feeder-free culture of human embryonic stem cells. Methods Enzymol. *420*, 37–49.

Antczak, C., Shum, D., Escobar, S., Bassit, B., Kim, E., Seshan, V.E., Wu, N., Yang, G., Ouerfelli, O., Li, Y.M., et al. (2007). High-throughput identification of inhibitors of human mitochondrial peptide deformylase. J. Biomol. Screen. *12*, 521–535.

Barberi, T., Bradbury, M., Dincer, Z., Panagiotakos, G., Socci, N.D., and Studer, L. (2007). Derivation of engraftable skeletal myoblasts from human embryonic stem cells. Nat. Med. *13*, 642–648.

Bendall, S.C., Stewart, M.H., Menendez, P., George, D., Vijayaragavan, K., Werbowetski-Ogilvie, T., Ramos-Mejia, V., Rouleau, A., Yang, J., Bosse, M., et al. (2007). IGF and FGF cooperatively establish the regulatory stem cell niche of pluripotent human cells in vitro. Nature *448*, 1015–1021.

Boyer, L.A., Lee, T.I., Cole, M.F., Johnstone, S.E., Levine, S.S., Zucker, J.P., Guenther, M.G., Kumar, R.M., Murray, H.L., Jenner, R.G., et al. (2005). Core transcriptional regulatory circuitry in human embryonic stem cells. Cell *122*, 947–956.

Chen, S., Do, J.T., Zhang, Q., Yao, S., Yan, F., Peters, E.C., Scholer, H.R., Schultz, P.G., and Ding, S. (2006). Self-renewal of embryonic stem cells by a small molecule. Proc. Natl. Acad. Sci. USA *103*, 17266–17271.

D'Amour, K.A., Agulnick, A.D., Eliazer, S., Kelly, O.G., Kroon, E., and Baetge, E.E. (2005). Efficient differentiation of human embryonic stem cells to definitive endoderm. Nat. Biotechnol. *23*, 1534–1541.

Dennis, G., Jr., Sherman, B.T., Hosack, D.A., Yang, J., Gao, W., Lane, H.C., and Lempicki, R.A. (2003). DAVID: Database for Annotation, Visualization, and Integrated Discovery. Genome Biol. *4*, 3. 10.1186/gb-2003-4-5-p3.

Ding, S., and Schultz, P.G. (2004). A role for chemistry in stem cell biology. Nat. Biotechnol. *22*, 833–840.

Ding, S., Wu, T.Y., Brinker, A., Peters, E.C., Hur, W., Gray, N.S., and Schultz, P.G. (2003). Synthetic small molecules that control stem cell fate. Proc. Natl. Acad. Sci. USA *100*, 7632–7637.

Esmaeili, F., Tiraihi, T., Movahedin, M., and Mowla, S.J. (2006). Selegiline induces neuronal phenotype and neurotrophins expression in embryonic stem cells. Rejuvenation Res. *9*, 475–484.

Ginis, I., Luo, Y.Q., Miura, T., Thies, S., Brandenberger, R., Gerecht-Nir, S., Amit, M., Hoke, A., Carpenter, M.K., Itskovitz-Eldor, J., and Rao, M.S. (2004). Differences between human and mouse embryonic stem cells. Dev. Biol. *269*, 360–380.

Hoffman, L.M., and Carpenter, M.K. (2005). Characterization and culture of human embryonic stem cells. Nat. Biotechnol. *23*, 699–708.

Laflamme, M.A., Chen, K.Y., Naumova, A.V., Muskheli, V., Fugate, J.A., Dupras, S.K., Reinecke, H., Xu, C.H., Hassanipour, M., Police, S., et al. (2007). Cardiomyocytes derived from human embryonic stem cells in pro-survival factors enhance function of infarcted rat hearts. Nat. Biotechnol. *25*, 1015–1024.

Levenstein, M.E., Ludwig, T.E., Xu, R.H., Llanas, R.A., VanDenHeuvel-Kramer, K., Manning, D., and Thomson, J.A. (2006). Basic fibroblast growth factor support of human embryonic stem cell self-renewal. Stem Cells *24*, 568–574.

Li, J., Wang, G., Wang, C., Zhao, Y., Zhang, H., Tan, Z., Song, Z., Ding, M., and Deng, H. (2007). MEK/ERK signaling contributes to the maintenance of human embryonic stem cell self-renewal. Differentiation *75*, 299–307.

O'Brien, J., Wilson, I., Orton, T., and Pognan, F. (2000). Investigation of the Alamar Blue (resazurin) fluorescent dye for the assessment of mammalian cell cytotoxicity. Eur. J. Biochem. *267*, 5421–5426.

Pera, M.F., Andrade, J., Houssami, S., Reubinoff, B., Trounson, A., Stanley, E.G., Ward-van Oostwaard, D., and Mummery, C. (2004). Regulation of human embryonic stem cell differentiation by BMP-2 and its antagonist noggin. J. Cell Sci. *117*, 1269–1280.

Perrier, A.L., Tabar, V., Barberi, T., Rubio, M.E., Bruses, J., Topf, N., Harrison, N.L., and Studer, L. (2004). From the cover: derivation of midbrain dopamine neurons from human embryonic stem cells. Proc. Natl. Acad. Sci. USA *101*, 12543–12548.

Sato, N., Sanjuan, I.M., Heke, M., Uchida, M., Naef, F., and Brivanlou, A.H. (2003). Molecular signature of human embryonic stem cells and its comparison with the mouse. Dev. Biol. *260*, 404–413.

Sato, N., Meijer, L., Skaltsounis, L., Greengard, P., and Brivanlou, A.H. (2004). Maintenance of pluripotency in human and mouse embryonic stem cells through activation of Wnt signaling by a pharmacological GSK-3-specific inhibitor. Nat. Med. *10*, 55–63.

Saxe, J.P., Wu, H., Kelly, T.K., Phelps, M.E., Sun, Y.E., Kornblum, H.I., and Huang, J. (2007). A phenotypic small-molecule screen identifies an orphan ligand-receptor pair that regulates neural stem cell differentiation. Chem. Biol. *14*, 1019–1030.

Tomishima, M.J., Hadjantonakis, A.K., Gong, S., and Studer, L. (2007). Production of green fluorescent protein transgenic embryonic stem cells using the GENSAT bacterial artificial chromosome library. Stem Cells *25*, 39–45.

Vallier, L., Alexander, M., and Pedersen, R.A. (2005). Activin/Nodal and FGF pathways cooperate to maintain pluripotency of human embryonic stem cells. J. Cell Sci. *118*, 4495–4509.

Watanabe, K., Ueno, M., Kamiya, D., Nishiyama, A., Matsumura, M., Wataya, T., Takahashi, J.B., Nishikawa, S., Nishikawa, S., Muguruma, K., and Sasai, Y. (2007). A ROCK inhibitor permits survival of dissociated human embryonic stem cells. Nat. Biotechnol. *25*, 681–686.

Wu, X., Ding, S., Ding, G., Gray, N.S., and Schultz, P.G. (2004a). Small molecules that induce cardiomyogenesis in embryonic stem cells. J. Am. Chem. Soc. *126*, 1590–1591.

Wu, X., Walker, J., Zhang, J., Ding, S., and Schultz, P.G. (2004b). Purmorphamine induces osteogenesis by activation of the hedgehog signaling pathway. Chem. Biol. *11*, 1229–1238.

Xu, C.H., Inokuma, M.S., Denham, J., Golds, K., Kundu, P., Gold, J.D., and Carpenter, M.K. (2001). Feeder-free growth of undifferentiated human embryonic stem cells. Nat. Biotechnol. *19*, 971–974.

Xu, R.H., Chen, X., Li, D.S., Li, R., Addicks, G.C., Glennon, C., Zwaka, T.P., and Thomson, J.A. (2002). BMP4 initiates human embryonic stem cell differentiation to trophoblast. Nat. Biotechnol. *20*, 1261–1264.

Ying, Q.L., Nichols, J., Chambers, I., and Smith, A. (2003). BMP induction of Id proteins suppresses differentiation and sustains embryonic stem cell self-renewal in collaboration with STAT3. Cell *115*, 281–292.

Zhang, J.H., Chung, T.D., and Oldenburg, K.R. (1999). A simple statistical parameter for use in evaluation and validation of high throughput screening assays. J. Biomol. Screen. *4*, 67–73.

Zhang, S.C., Wernig, M., Duncan, I.D., Brustle, O., and Thomson, J.A. (2001). In vitro differentiation of transplantable neural precursors from human embryonic stem cells. Nat. Biotechnol. *19*, 1129–1133.